Entelon® (*vitis vinifera* seed extract) reduces inflammation and calcification in a beagle dog model of intravascular bovine pericardium implantation

Gab-Chol Choi[1,2#], Sokho Kim[1,3#], Md. MAHBUBUR Rahman[1,3], Ji Hyun Oh[1], MS, Yun Seok Cho[1], PhD, Hong Ju Shin[1*], MD, PhD

[1]Department of Thoracic and Cardiovascular Surgery, Korea University Ansan Hospital, Korea University College of Medicine, Ansan, Korea

[2]Animal Medical Center W, 46 Worldcup-ro, Mapo-gu, Seoul, Korea

[3]KNOTUS Co., Ltd., Research Center, Incheon, Korea

[#]Authors contributed equally as co-first author

Corresponding Author Contact Information:

Hong Ju Shin, MD, PhD

Department of Thoracic and Cardiovascular Surgery, Korea University Ansan Hospital, Korea University College of Medicine, Ansan, Korea

Tel: 82-10-6282-9704

E-mail: babymedi@naver.com

Keywords: bovine pericardium, Entelon150®, grape seed extract, calcification

Total Word Count: 2,632

Abstract

Objective: Inflammation and calcification are major factors responsible for failure of bioprosthetic valve and other substitute heart valve implantations. The objective of this study was to evaluate the anti-inflammatory and anti-calcification effects of Entelon150® (consisting of grape-seed extract) in a beagle dog model of intravascular bovine pericardium implantation.

Methods: In total, 8 healthy male beagle dogs were implanted with a bovine pericardium bilaterally in the external jugular veins and divided into two groups. Animals in the Entelon150® group (n = 4) were treated with 150 mg of Entelon150® twice daily for six weeks after surgery. The negative control (NC) group (n = 4) was treated with 5 ml of saline using the same method. After six weeks, we measured the calcium content, performed histological examination, and performed molecular analysis.

Results: The calcium content of implanted tissue in the Entelon150® group (0.56±0.14 mg/g) was significantly lower than that in the NC group (1.48±0.57 mg/g) ($p < 0.05$). Histopathological examination showed that infiltration of chronic inflammatory cells, such as fibroblasts and macrophages, occurred around the graft in all groups; however, the inflammation level of the implanted tissue in the Entelon150® group was significantly lower than that in the NC group. Both immunohistochemical and western blot analyses revealed that bone morphogenetic protein 2 expression was significantly attenuated in the Entelon150® group.

Conclusions: Our results indicate that Entelon150® significantly attenuates post-implantation inflammation and degenerative calcification of the bovine pericardium in dogs. Therefore, Entelon150® may increase the longevity of the bovine pericardium after intravascular implantation.

Introduction

Bovine pericardium is widely used in patch material during vascular surgery. It is also used in bioprosthetic heart valve leaflets with specific treatment to increase its longevity. Heart valves made of a bovine pericardium are safe, offer improved hemodynamics, have less risk of thrombosis, and do not need long-term anticoagulant therapy [1,2]. However, the durability of the bovine pericardium is a major problem, as it is prone to valve calcification, structural deterioration, and eventual failure. Several approaches to reduce calcification have been attempted, including systemic anti-calcification agent administration. However, many of these approaches have been either ineffective or have produced unwanted side effects [3]. To overcome this drawback, studies on the complementary treatment of calcification have focused on traditional herbal medicines recently [4-6].

Grape fruit (*Vitis vinifera*) is one of the most important and popular fruit crops worldwide because of its high phytochemical content and its nutritional value. All parts of this fruit have been used as dietary supplements to treat or prevent various diseases [7-9]. In general, grape fruit is rich in phenols, flavonoids, and fatty acids. The anti-inflammatory [7,9] and anti-oxidative [7] effects of grape seed extract (GSE) are now well established.

Interleukin-6 (IL-6) plays an important role in increasing bone morphogenic protein 2/4 (BMP-2/4) expression in vessels and valve tissue, thereby leading to vascular calcification [3]. It has been shown that application of GSE reduces IL-6 activity in different disease models [10,11].

To the best of our knowledge, there have been no studies examining the effects of GSE on bovine pericardium implants. It is thus unknown whether GSE could prevent bovine pericardium calcification and degeneration. Therefore, the purpose of this study was to investigate the anti-inflammatory and anti-calcification effects of Entelon150® on intravenous bovine pericardium implants in beagle dogs.

Methods

Animal and experimental design

Eight healthy male beagle dogs (20 weeks old; mean body weight 9.76 ± 0.32 kg, range 8.00–10.80 kg) were used in this study. They were housed separately in stainless steel cages (W 895 × L 795 × H 765 mm) in an environmentally controlled room (temperature 23 ± 3 ℃, relative humidity 55 ± 15%, ventilation frequency 10-20 times/hr, light cycle 8 am to 8 pm, illumination 150 to 300 Lux). Food and sterilized water were available ad libitum. Animals were divided equally into two groups: 1) Negative control (NC) group: vehicle-treated after prosthetic implantation; 2) Entelon150®-treated group: treated with grape seed extract (Entelon150®; Hanlim Pharm. Co., Ltd. Yongin-si, Korea), 150 mg per animal twice daily for six weeks after implantation. The mouth of the animal was opened to its natural position in the breeding box, and the test article was placed on the tongue. The animal's mouth was then shut, and the neck was gently stroked until the animal swallowed. All animals were closely monitored during the experimental period, and we observed no clinical symptoms. This study was approved by the Institutional Animal Care and Use Committee at the KNOTUS Co., Ltd., Incheon-si, Korea (Certificate No: IACUC 19-KE-132).

Surgical procedure for implantation and postoperative care

Each animal was anesthetized with an intravenous injection of Zoletil 50 (VIRBAC, France; 5 mg/kg) and xylazine (Rompun®, Bayer AG, Germany; 2.5 mg/kg). After intubation with a 3.0-mm endotracheal tube, inhaled isoflurane was used to maintain anesthesia. All animals received 0.9% saline (10 ml/kg/h) intravenously throughout the surgical procedure. The skin was incised along the ventral cervical midline, and blunt separation was performed to expose the left external jugular vein from the sternohyoid muscle. After administration of heparin (50 IU/kg, IV), the left jugular vein was temporarily blocked using 4-0 silk and 5 French feeding

tubes. An 8-mm longitudinal incision was then made in the jugular vein using a no. 11 surgical blade. A commercially available bovine pericardium (PERIBORN® Bovine Pericardium, BP0506, Taewoong Medical Co., Ltd. Gimpo-si, South Korea) was used in this study. Before implantation, the Bovine pericardium was rinsed for 30 min in 500 ml of sterile physiological saline. The antibiotic cephradine (30 mg/kg i.v, bid) and the analgesic tramadol (2 mg/kg i.v., tid) were injected for three days after surgery. An approximately 3-mm rectangular bioprosthetic was fixed to the inner wall of the jugular vein using a 6-0 polypropylene running suture. The jugular vein was closed by angioplasty using a 6-0 polypropylene running suture. The bovine pericardium was also implanted into the right external jugular vein as described above. The schematic diagram below shows the anatomy of the jugular vein in beagle dogs, relevant to this surgical procedure (Fig 1).

Measurement of vascular patency

Vascular patency was checked using the color doppler mode of an ultrasonic device (LOGIQ e Ultrasound; GE Healthcare, Fairfield, USA). Angiography was also performed with a bolus intravenous injection of 2 ml/kg iohexol (Omnipaque™, 300 mg I/ml; GE Healthcare) using a CT-scanner (CT; 16-channel multidetector; BrightSpeed Elite, GE Healthcare, Fairfield, CT, USA) for additional confirmation.

Sample collection

Six weeks after surgery and immediately after measuring vascular patency, the animals were euthanized and both the left and right external jugular veins were removed. The right external jugular vein was cleaned of connective tissues around the implanted prosthetic. The prosthetic was then stored in a cryogenic freezer maintained at about -80 ° C for later calcium quantification. Half of the left external jugular vein was fixed in a 10% neutral buffered formalin solution for histopathological examination, and the other half was stored in a

cryogenic freezer maintained at -80 ° C for western blotting.

Measurement of calcium content

Moisture was removed from the stored implant through 24 h of freeze-drying. After weighing the implants, they were suspended in a beaker containing 5 ml of aqua regia solution. Hydrogen peroxide (H_2O_2; 5 ml) was then added to the beaker, and the beaker was slowly heated to 70–80°C on a hot plate for 6 h to dissolve the tissue. The solution was then heated for a further 5 h at 140–150°C. An additional 5 ml of H_2O_2 was then added. Subsequently, each sample was diluted to a total volume of 50 ml with distilled water. The diluted samples were used to measure the calcium content.

Histopathological examination

For histopathological examination, each sample was soaked in 10% neutralized buffered formalin and processed using standard methods. Paraffin-embedded tissue was sliced into 4-μm-thick sections and stained with hematoxylin and eosin (H & E). For H & E-stained slides, infiltration of inflammatory cells around the implanted bovine pericardium was quantified according to the following criteria: 0: none, 1: weak inflammatory cell infiltration, 2: moderate inflammatory cell infiltration, 3: severe inflammatory cell infiltration.

For immunohistochemical analysis, the sections were deparaffinized following standard protocols. The sections were then incubated in 3% hydrogen peroxide for 10 min to inactivate endogenous peroxidase and then blocked by incubating the sections for 1 h in 5% bovine serum albumin. The sections were then incubated overnight with anti-alpha smooth muscle actin (α-SMA) (1:1600, ab5964, Abcam) and bone morphogenetic protein 2 (BMP-2) (1:200, orb251474, Biorbyt) primary antibodies at 4°C. The sections were washed and incubated with secondary anti-rabbit (α-SMA) or anti-mouse (BMP-2) antibodies for 30 min at approximately

20°C. The sections were then washed, counterstained with Mayers Hematoxylin, and mounted on slides. The percentage of stained area (%) was compared between groups. For immunohistochemically stained slides, the expression area was analyzed using a slide scanner (Axio Scan Z1, Carl Zeiss, Germany), and the slides were then subjected to image analysis (ZEN, Carl Zeiss, Germany).

Western blotting

Cryogenically frozen samples were homogenized using RIPA buffer, after which proteins were extracted and quantified. A sample for electrophoreses was prepared by quantifying the sample's protein content, and the sample was electrophoresed on 10-14% acrylamide gel for 120 minutes. The protein was then transferred to a polyvinylidene difluoride (PVDF) membrane, and non-specific protein binding sites were removed using blocking buffer. The PVDF membrane was incubated with interleukin-6 (IL-6), osteopontin (OPN), and bone morphogenetic protein 2 (BMP-2) primary antibodies at about 4°C for 6 hours or more. After the primary antibody reaction, the membrane was exposed to the secondary antibody (diluted 1: 10,000). After the reaction was complete, the cells were washed with PBS-T buffer (0.5% Tween 20 in phosphate buffered saline) and the sample was developed using an enhanced chemiluminescence (ECL) reagent for immunoblot analysis. The color-completed sample was analyzed using an image analyzer. β-actin was used as intrinsic control. Finally, the ECL signal was quantitated using the pixel density analysis algorithm within ImageJ software (National Institute of Health, NY, USA). The relative band density was calculated as follows: relative band density = (specific band density/β-actin band density) × 100.

Statistical analysis

All data are expressed as mean ± SD. Statistical analyses were performed using GraphPad Prism 5.0 software (GraphPad Software, Inc., San Diego, CA, USA). An unpaired t-test was

used to compare two groups. All statistical tests were two-sided, and significance was defined as $P < 0.05$.

Results

There were no differences in body weight between the control and Entelon150®-treated groups (Fig 2 A). Vascular patency was evaluated using ultrasonography and CT scanning. No interruption of flow patency was observed on either CT scans (Fig 2, B and C) or ultrasonographs (Fig 3).

Calcified lesions were not observed around the vessel or in the implants in either control or Entelon150®-treated groups. The Ca^{2+} level in the Entelon150®-treated group (0.56±0.14 mg/g) was significantly lower than that in the NC group (1.48±0.57 mg/g) ($P < 0.05$, Fig 4). Western blot analysis showed that BMP-2 levels in the Entelon150®-treated group (82.21±11.20%) were significantly lower ($P < 0.001$) than in the NC group (100.00±4.63%). Western blot analysis also revealed that IL-6 levels in the Entelon150®-treated group (55.36±5.49%) were significantly lower ($P < 0.001$) than NC group (100.00±10.30%). However, the expression of OPN was not significantly different between two groups (Fig 5). Histopathological examination revealed infiltration of chronic inflammatory cells such as fibroblasts and macrophages around the graft in all groups. However, the inflammation level of the Entelon150®-treated group (1.50±0.58%) was significantly lower ($P < 0.001$) than the NC group (2.25±0.96%). In particular, a basophilic substance presumed to be the earliest sign of calcium deposition was observed in the NC group between the intercellular matrixes of the peri-graft tissue (Fig 6). Immunohistochemical staining revealed that BMP-2 levels in the Entelon150®-treated group (1.27±0.06%) were significantly ($P < 0.05$) lower than those in the NC group (1.67±0.31%). However, the expression of α-SMA was not significantly

different between the two groups (Fig 7).

Discussion

This study was the first to investigate the anti-inflammatory and anti-calcification effects of Entelon150® using a beagle dog model of intravenous bovine pericardium implantation. Chronic inflammation and calcification are major signs of the structural deterioration, dysfunction, and failure of bioprosthetic valve made of bovine pericardium [3,12,13]. We hypothesized that Entelon150® would reduce the expression of inflammatory cytokines in the vascular tissue of bovine pericardial implants, thereby suppressing calcification and bovine pericardium. In this study we demonstrated that Entelon150® treatment had two effects: significantly attenuating both inflammation and calcification in a beagle dog model of intravascular bovine pericardial implantation.

Indeed, immunological rejection of heterologous tissue is a challenging medical problem contributing to post-implant xenograft degeneration [14]. Our histopathological results are consistent with previous studies observing infiltration of chronic inflammatory cells such as fibroblasts and macrophages around the graft. The inflammation levels of the Entelon150®-treated group was significantly lower than the negative control group. In addition, a basophilic substance, presumed to be the earliest sign of calcium deposition, was observed between the intercellular matrixes of the peri-graft tissue in the negative control group. The basophilic staining using the H & E stain method indicated calcium deposition [15]. The results suggest that administration of Entelon150® lowered inflammation levels and inhibited calcium deposition in the tissues surrounding the graft.

In addition, we found that bovine pericardium triggered an immunological response, as we

observed a significant elevation of IL-6 in the NC group. Steroidal anti-inflammatory therapy significantly reduces the incidence of postoperative valve tissue rejection in patients, indicating that suppressing the valve-induced immunological response may improve the postoperative durability of bioprosthetic aortic valve implants [16]. Importantly, our data showed that Entelon150® treatment significantly lowered IL-6 levels, thus mitigating inflammation.

BMP-2 is a member of the transforming growth factor (TGF) superfamily and is known to be a master regulator of conventional and ectopic osteogenesis [17]. Alteration of BMP-2 reportedly aggravates skeletal and extraskeletal mineralization [18]. In addition, BMP-2 plays a critical role in vascular disease, including atherosclerosis and plaque instability through its effects on vascular inflammation. BMP-2 also regulates vascular oxidative stress and vascular calcification by stimulating osteogenesis in vascular smooth muscle cells [19]. Furthermore, IL-6 activity is strongly associated BMP-2 expression [3,12] and calcification [20]. In this study we found that calcium content and IL-6 expression were significantly lowered in the bovine pericardium of the Entelon150®-treated group. To elucidate the underlying mechanism involved, we evaluated BMP-2 expression in implanted tissue. Interestingly, Entelon150® treatment significantly lowered BMP-2 expression, demonstrating its therapeutic molecular effects. OPN is an extracellular matrix glycoprotein mainly taking part in bone morphogenesis, bio-mineralization and calcification. OPN is produced as a cytokine in activated T cells and macrophages, demonstrating that OPN plays an important role modulating inflammation. During the healing process or under pro-inflammatory conditions, OPN expression is elevated near inflammatory cells. OPN is reportedly associated with inflammation, atherosclerosis, and vascular calcification [21]. We also found that along with IL-6 and calcification, OPN expression was increased in the implanted tissue and was non significantly lowered by Entelon150® administration. Additionally, α-SMA expression is used as a measure of tissue fibrosis. Calcification and fibrosis have many common features such as risk factors and have

235 histopathological lesions with similar pathogenic pathways and mediators. The factors
236 initiating calcification include inflammation, cell injury, and tissue infiltration by inflammatory
237 cells, lipids, cytokines, and reactive oxygen species and the overexpression of α-SMA in
238 calcified tissue has also been reported [22,23]. Consistent with these findings, the expression
239 α-SMA in the bovine pericardium was lowered by Entelon150® treatment; however, this
240 difference was not statistically significant.

241 We have previously found that the angiotensin II type 1 receptor blocker losartan attenuates
242 bioprosthetic valve leaflet calcification in a rabbit model of intravascular implantation [3].
243 Calcification of bovine pericardium appears unrelated to certain mechanisms, but rather
244 appears related to reduced inflammation and substances like IL-6, BMP-2, and OPN. Any
245 substance that lowers inflammation through IL-6, BMP-2, and OPN may help prevent
246 calcification. From this point of view, Entelon150®, which consists of grape seed extract, will
247 be more powerful than other synthetic medications at preventing calcification.

248 **Limitations**

249 The limitations of this study are its relatively low number and the uncertain mechanism of
250 degenerative calcification in our beagle dog model of intravascular bovine pericardium
251 implantation. It is unclear whether the mechanisms in our model are similar to the mechanisms
252 underlying calcification of bovine perciardium in humans. However, we previously compared
253 five implantation methods in a rabbit model and found that the intravenous implantation model
254 most closely resembled bioprosthetic valve made of bovine pericardium calcification in
255 humans. Furthermore, we reported that the calcium content was higher in intravenous implants
256 than in arterial patch implants [24]. We performed our experiments in beagle dogs rather than
257 rabbits; however, we think our results are consistent with the findings in our rabbit intravascular
258 model.

Conclusion

We found that Entelon 150® significantly attenuated post-implant degenerative calcification in a beagle dog of intravascular bovine pericardium implantation model. Further observations are required to assess the effects of Entelon 150® on native vessel calcification in another animal model.

Conflict of Interest Statement: The authors report no conflicts of interest.

Funding: This study was supported by a Korea University Grant (K1924931).

AUTHOR CONTRIBUTIONS

Conceptualization: Ji Hyun Oh, Yun Seok Cho, Hong Ju Shin.
Data curation: Sokho Kim.
Formal analysis: Md. MAHBUBUR Rahman.
Investigation: Sokho Kim, Hong Ju Shin.
Methodology: Gab-Chol Choi, Sokho Kim, Md. MAHBUBUR Rahman, Hong Ju Shin.
Supervision: Yun Seok Cho, Hong Ju Shin.
Writing – original draft: Gab-Chol Choi, Sokho Kim, Md. MAHBUBUR Rahman.
Writing – review & editing: Ji Hyun Oh, Yun Seok Cho, Hong Ju Shin.
Gab-Chol Choi and Sokho Kim contributed equally to this article and share co-first authorship.

283 **References:**

284 1. Soares JS, Feaver KR, Zhang W, Kamensky D, Aggarwal A, Sacks MS. Biomechanical
285 behavior of bioprosthetic heart valve heterograft tissues: characterization, simulation, and
286 performance. Cardiovasc Eng Technol 2016;7:309-351.

287 2. Lee S, Levy RJ, Christian AJ, Hazen SL, Frick NE, Lai EK, et al. Calcification and
288 Oxidative Modifications Are Associated With Progressive Bioprosthetic Heart Valve
289 Dysfunction. J Am Heart Assoc 2017;6:e005648.

290 3. Shin HJ, Kim D-H, Park HK, Park YH. The angiotensin II type 1 receptor blocker losartan
291 attenuates bioprosthetic valve leaflet calcification in a rabbit intravascular implant model.
292 Eur J Cardiothorac Surg 2016;50:1045-52.

293 4. Wang J, Qiu X, Xu T, Sheng Z, Yao L. Sclerostin/Receptor related protein 4 and ginkgo
294 biloba extract alleviates β-glycerophosphate-induced vascular smooth muscle cell
295 calcification by inhibiting Wnt/β-Catenin pathway. Blood Purif 2019;47:17-23.

296 5. Liao L, Zhuang X, Li W, Su Q, Zhao J, Liu Y. Polysaccharide from Fuzi protects against
297 Ox-LDL-induced calcification of human vascular smooth muscle cells by increasing
298 autophagic activity. Mol Med Rep 2018;17:5109-15.

299 6. Freise C, Kim KY, Querfeld U. A Lindera obtusiloba extract blocks calcium-/phosphate-
300 induced transdifferentiation and calcification of vascular smooth muscle cells and
301 interferes with matrix metalloproteinase-2 and metalloproteinase-9 and NF-κB. Evid
302 Based Complement Alternat Med 2015;2015:679238.

303 7. Ma ZF, Zhang H. Phytochemical constituents, health Benefits, and industrial applications
304 of grape seeds: a mini-review. Antioxidants (Basel) 2017;6: E71.

8. Arora P, Ansari SH, Najmi AK, Anjum V, Ahmad S. Investigation of anti-asthmatic potential of dried fruits of Vitis vinifera L. in animal model of bronchial asthma. Allergy Asthma Clin Immunol 2016;12:42.

9. Park JS, Park MK, Oh HJ, Woo YJ, Lim MA, Lee JH, et al. Grape-seed proanthocyanidin extract as suppressors of bone destruction in inflammatory autoimmune arthritis. PLoS One 2012;7:e51377.

10. Zhang Y, Shi H, Wang W, Ke Z, Xu P, Zhong Z, et al. Antithrombotic effect of grape seed proanthocyanidins extract in a rat model of deep vein thrombosis. J Vasc Surg 2011;53:743-53.

11. Wang H, Xue Y, Zhang H, Huang Y, Yang G, Du M, et al. Dietary grape seed extract ameliorates symptoms of inflammatory bowel disease in IL10-deficient mice. Mol Nutr Food Res 2013;57:2253-7.

12. Lee S, Kim DH, Youn YN, Joo HC, Yoo KJ, Lee SH. Rosuvastatin attenuates bioprosthetic heart valve calcification. J Thorac Cardiovasc Surg 2019;158:731-41.

13. Soto ME, Salas JL, Vargas-Barron J, Marquez R, Rodriguez-Hernandez A, Bojalil-Parra R, et al. Pre- and post-surgical evaluation of the inflammatory response in patients with aortic stenosis treated with different types of prosthesis. BMC Cardiovasc Disord 2017;17:100.

14. Lorusso R, Corradi D, Maestri R, Bosio S, Curulli A, Beghi C, et al. Atorvastatin attenuates post-implant tissue degeneration of cardiac prosthetic valve bovine pericardial tissue in a subcutaneous animal model. Int J Cardiol 2010;141:68-74.

15. McCartney E, Squier W. Patterns and pathways of calcification in the developing brain. Dev Med Child Neurol 2014;56:1009-15.

16. Eishi K, Ishibashi-Ueda H, Nakano K, Kosakai Y, Sasako Y, Kobayashi J, et al. Calcific degeneration of bioprosthetic aortic valves in patients receiving steroid therapy. J Heart Valve Dis 1996;5:668-72.

17. Zhang M, Sara JD, Wang FL, Liu LP, Su LX, Zhe J, et al. Increased plasma BMP-2 levels are associated with atherosclerosis burden and coronary calcification in type 2 diabetic patients. Cardiovasc Diabetol 2015;14:64.

18. Nguyen-Yamamoto L, Tanaka KI, St-Arnaud R, Goltzman D. Vitamin D-regulated osteocytic sclerostin and BMP2 modulate uremic extraskeletal calcification. JCI Insight 2019;4(13). pii:126467.

19. Li X, Yang HY, Giachelli CM. BMP-2 promotes phosphate uptake, phenotypic modulation, and calcification of human vascular smooth muscle cells. Atherosclerosis 2008;199:271-7.

20. Lopez-Mejias R, Gonzalez-Gay MA. IL-6: linking chronic inflammation and vascular calcification. Nat Rev Rheumatol 2019;15:457-9.

21. Cho HJ, Cho HJ, Kim HS. Osteopontin: A multifunctional protein at the crossroads of inflammation, atherosclerosis, and vascular calcification. Curr Atheroscler Rep 2009;11:206-13.

22. Xu S, Liu AC, Gotlieb AI. Common pathogenic features of atherosclerosis and calcific aortic stenosis: role of transforming growth factor-beta. Cardiovasc Pathol 2010;19:236-47.

23. Latif N, Sarathchandra P, Chester AH, Yacoub MH. Expression of smooth muscle cell markers and co-activators in calcified aortic valves. Eur Heart J 2015;36:1335-45.

24. Kim D, Park HK, Park YH, Lee SH, Joo HC, Lee S, et al. Degenerative calcification of pericardial bioprostheses: comparison of five implantation methods in a rabbit model. J Heart Valve Dis 2015;24:621-8.

Figure Legends

Figure 1. Anatomical diagram of a beagle's jugular vein during the implantation procedure.

Figure 2. Effects of bioprosthetic valve implantation and Entelon® treatment on body weight and vascular patency as measured by CT-Scan.

Data are reported as mean ±SEM. NC: Negative control group, Entelon®: Entelon®-treated group. There are no significant differences between experimental groups.

Figure 3. Effects of bioprosthetic valve implantation and Entelon® treatment on vascular patency as measured by ultrasonography.

NC: Negative control group. Entelon®: Entelon®-treated group. The fluent vascular patency was confirmed by Ultrasonography.

Figure 4. Therapeutic efficacy of Entelon® treatment on the calcium content in bioprosthetic valve implants.

NC: Negative control group, Entelon®: Entelon®-treated group. The data are reported as mean ± SD. *: $p < 0.05$; and ***: $p < 0.001$, Bonferroni post hoc test following one-way ANOVA versus the NC group.

376 F**igure 5.** Effects of bioprosthetic valve implantation and Entelon® treatment on the protein
377 expression of BMP-2, IL-6 and OPN as analyzed by Western blot. β-Actin was used as an
378 internal control.

379 NC: Negative control group, Entelon®: Entelon®-treated group. IL-6: Interleukin-6, OPN:
380 osteopontin, BMP-2: bone morphogenetic protein 2. The data are reported as mean ± SD. *: p
381 < 0.05; and ***: p < 0.001, Bonferroni post hoc test following one-way ANOVA versus the
382 NC group.

383

384 F**igure 6.** Evaluation of the therapeutic efficacy of Entelon® using histological images
385 analysis. NC: Negative control group, Entelon®: Entelon®-treated group. The data are
386 reported as mean ± SD. ***: p < 0.001, Bonferroni post hoc test following one-way ANOVA
387 versus the NC group.

388

389 **Figure 7.** Evaluation of the therapeutic efficacy of Entelon® using histological images
390 analysis. NC: Negative control group, Entelon®: Entelon®-treated group. The data are
391 reported as mean ± SD. *: p < 0.05, Bonferroni post hoc test following one-way ANOVA
392 versus the NC group.

393

394

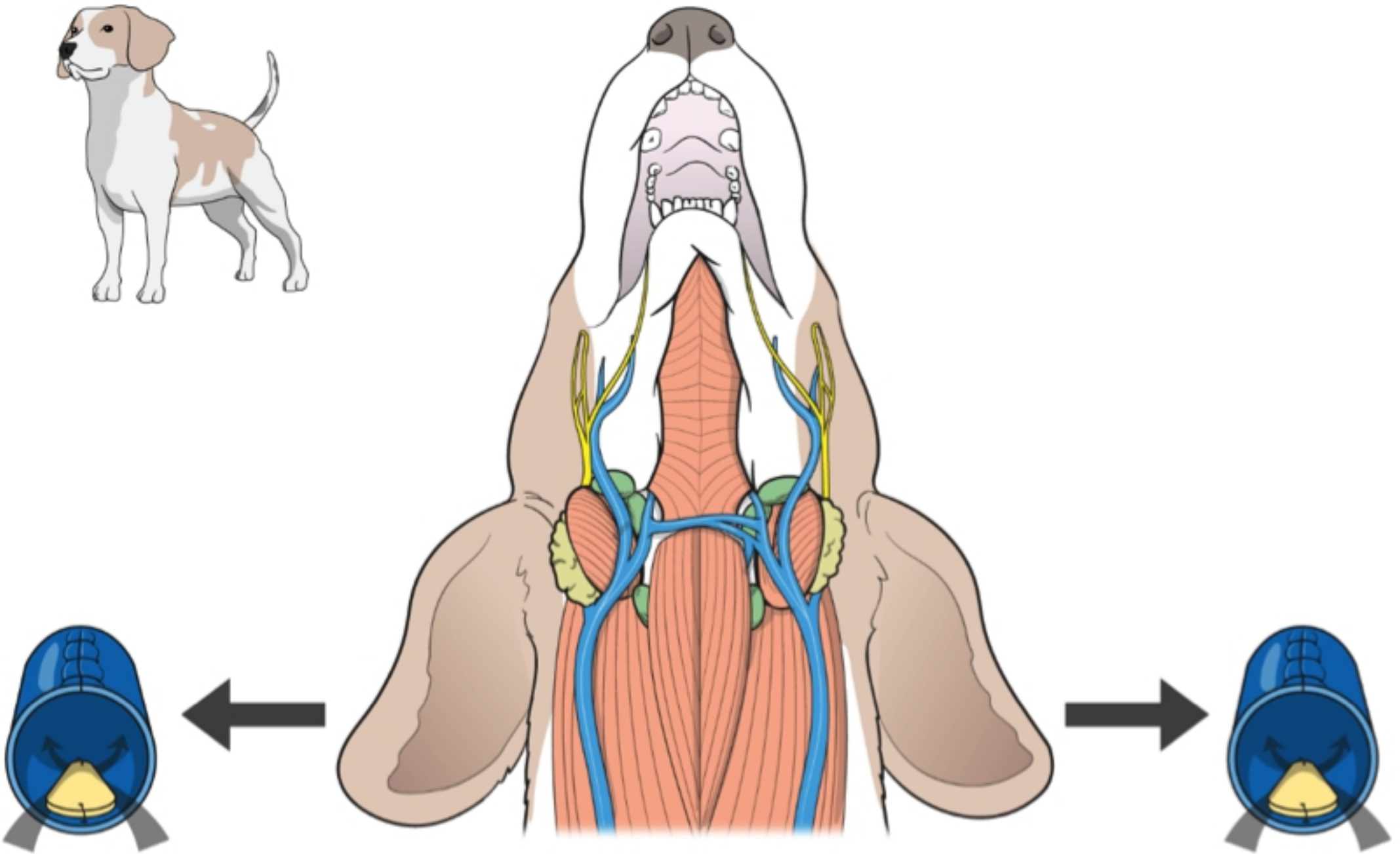

Figure 1

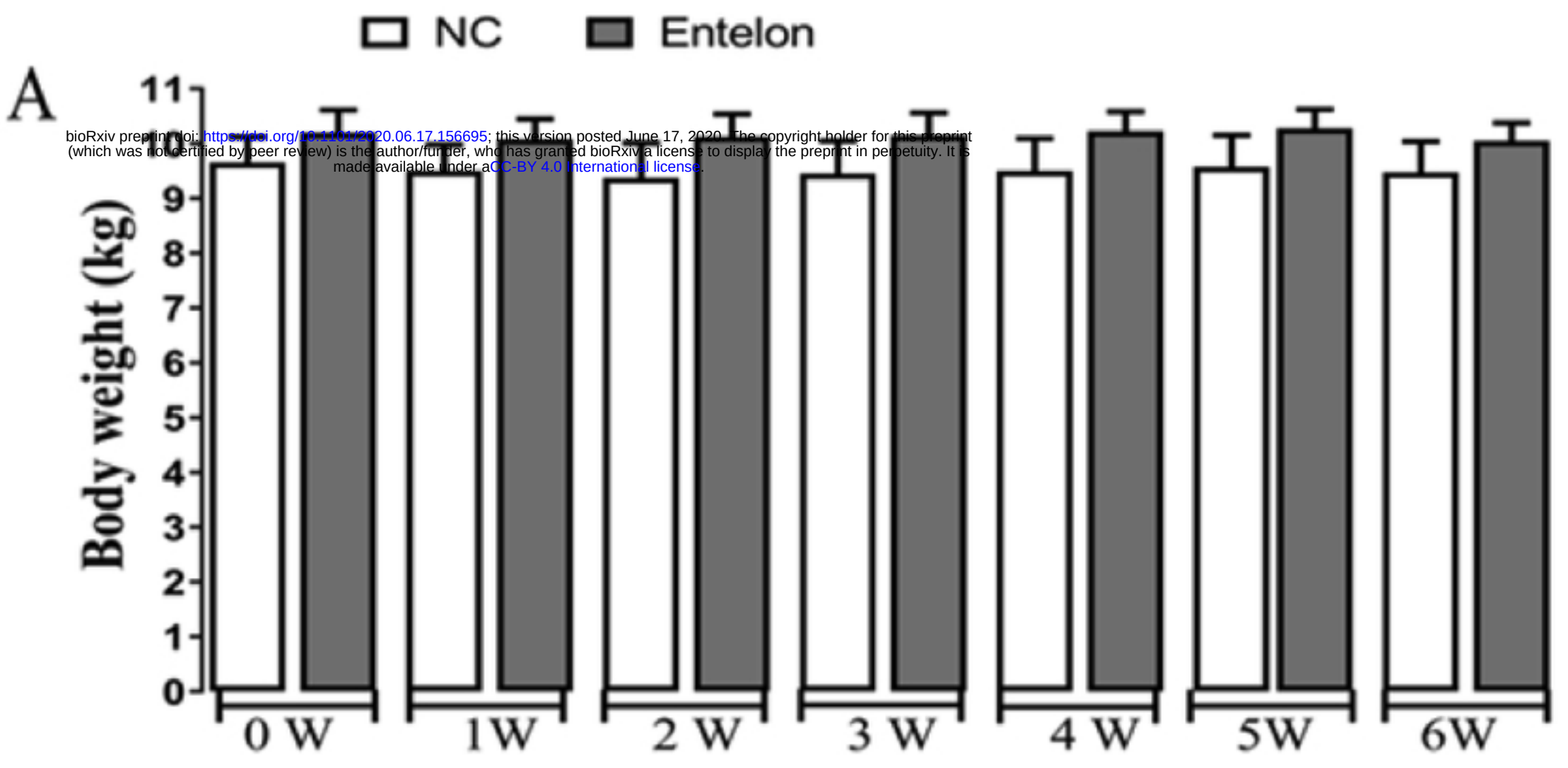

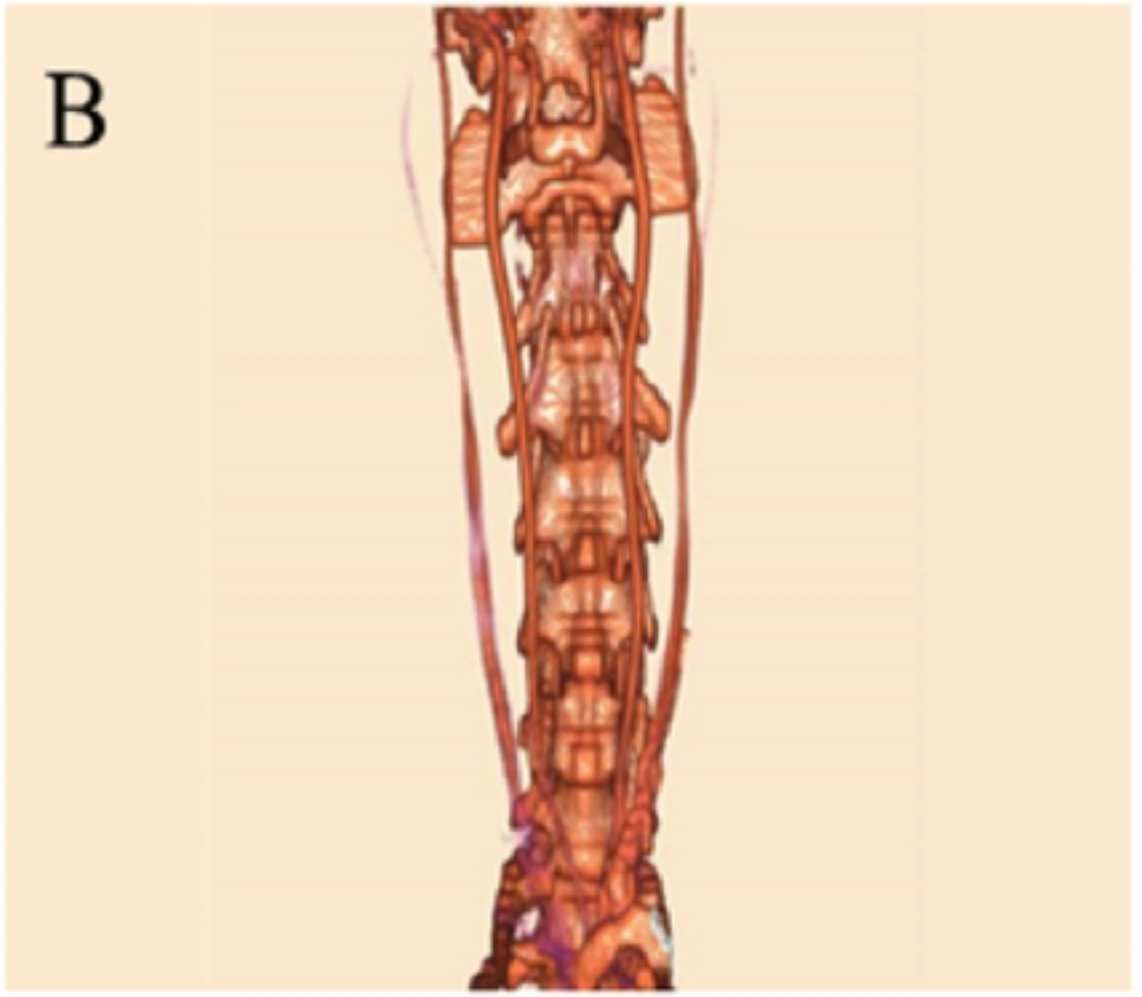

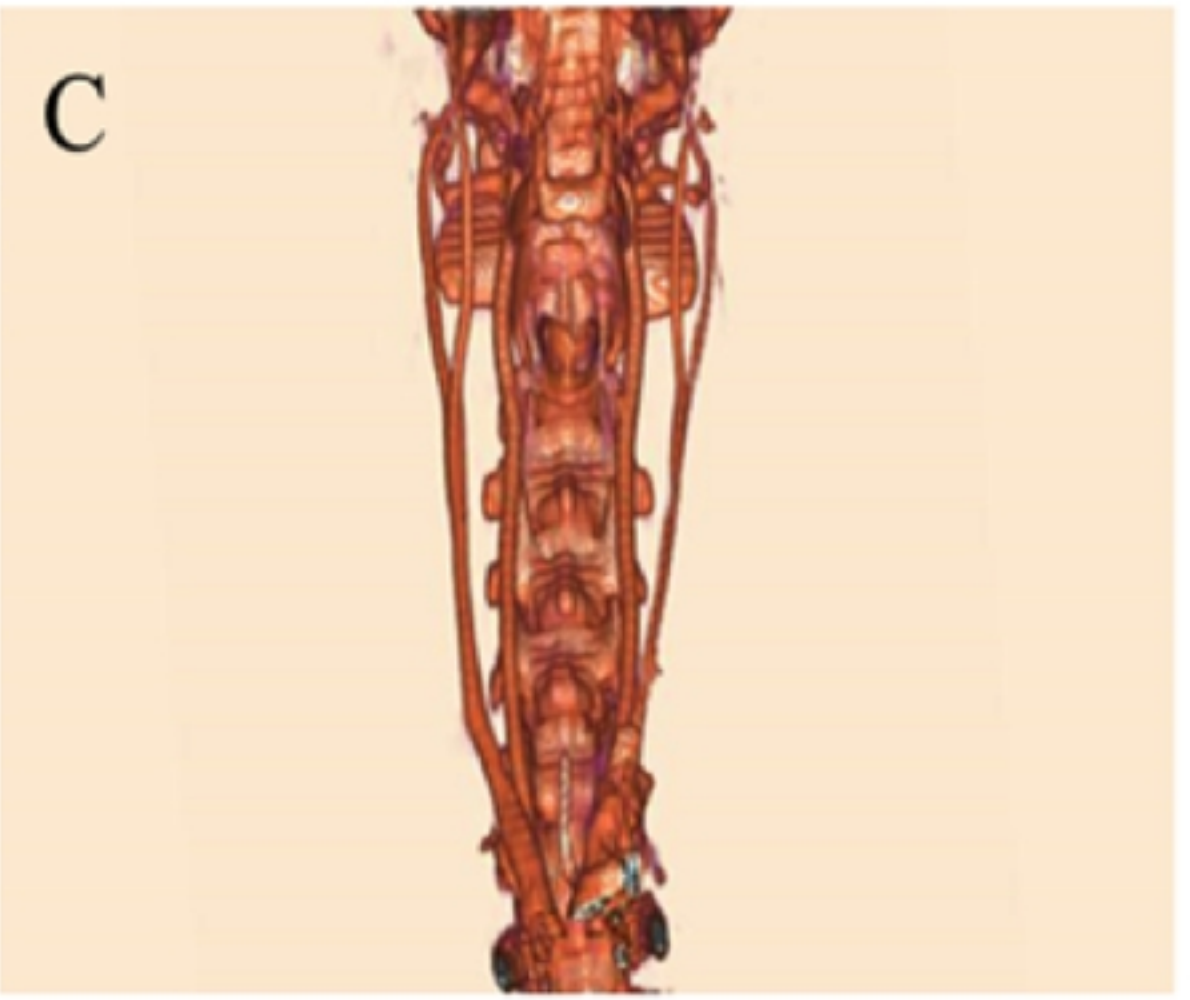

NC

Entelon

Figure 2

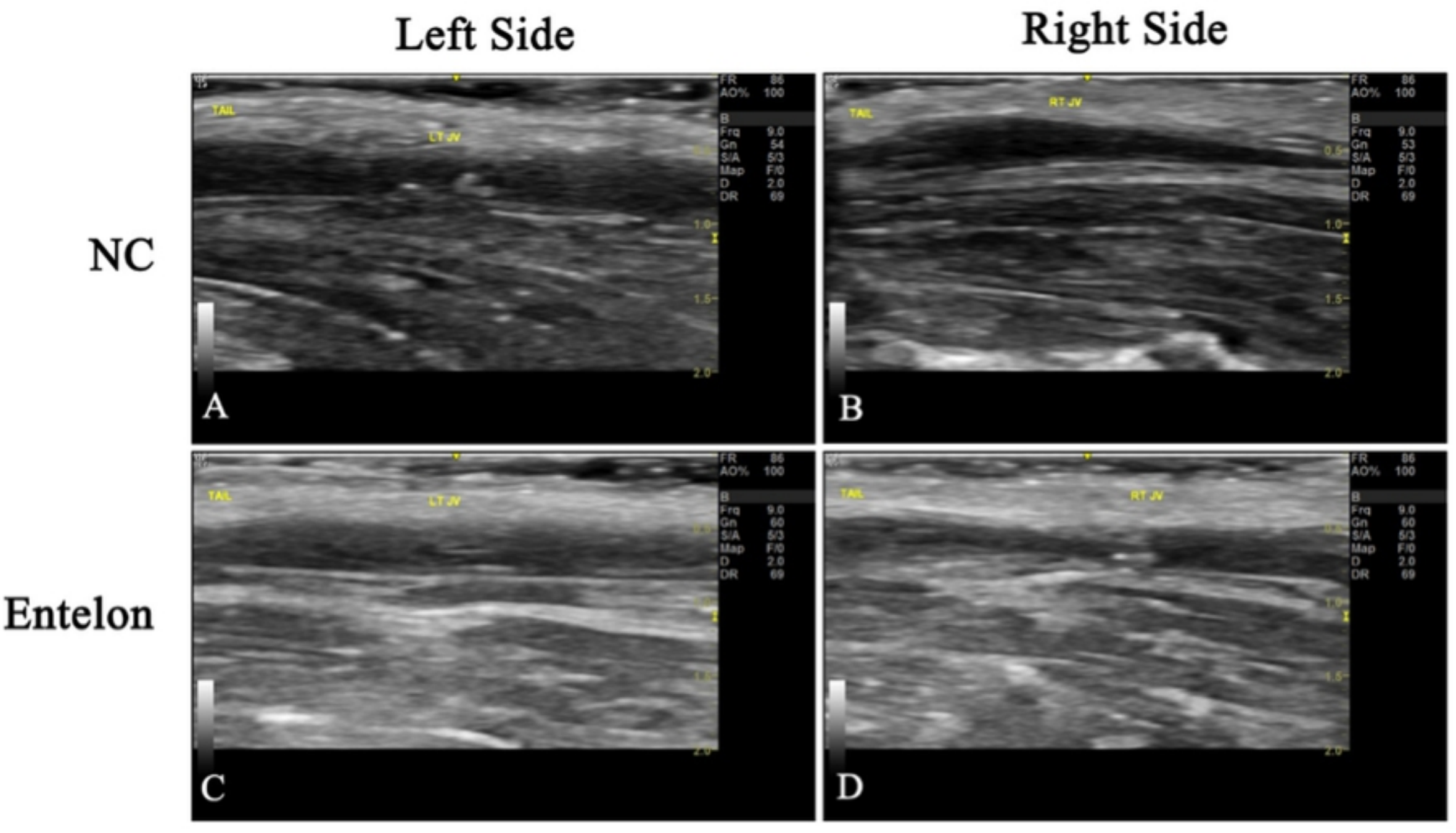

Figure 3

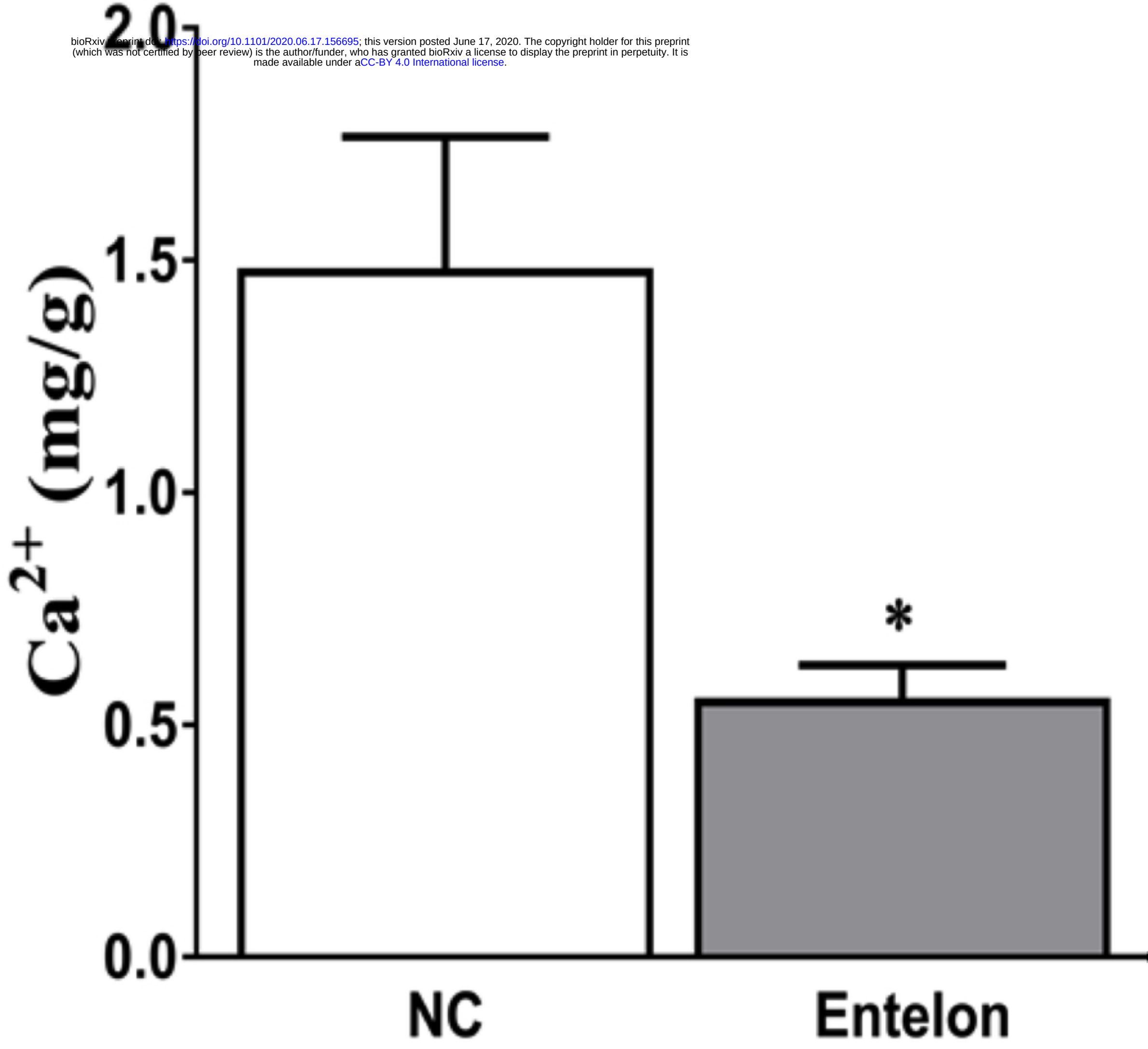

Figure 4

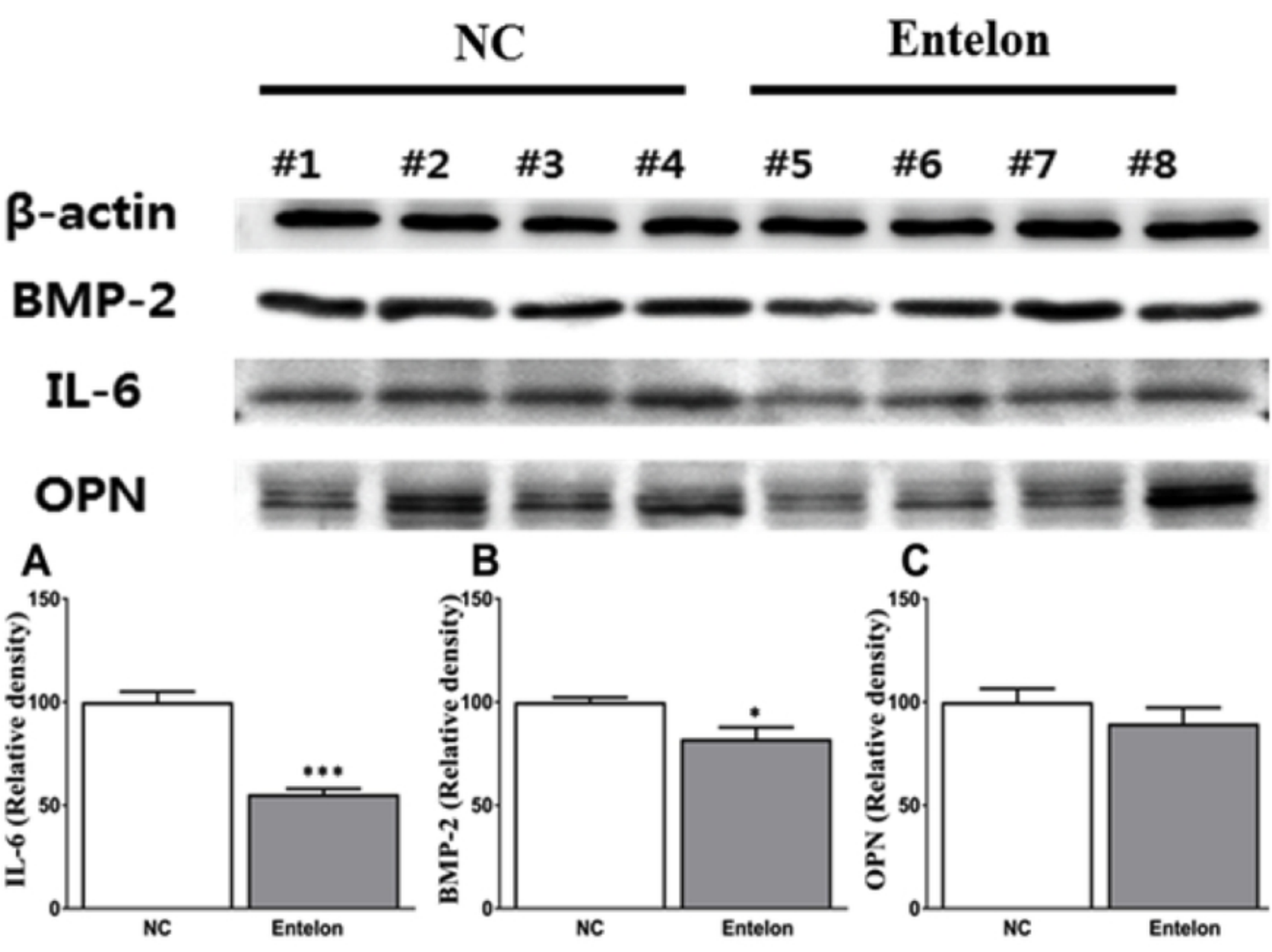
NC
Entelon
#1
#2
#3
#4
#5
#6
#7
#8
β-actin
BMP-2
IL-6
OPN
A
B
C
IL-6 (Relative density)
BMP-2 (Relative density)
OPN (Relative density)
150
100
50
0
***
*
NC
Entelon

Figure 5

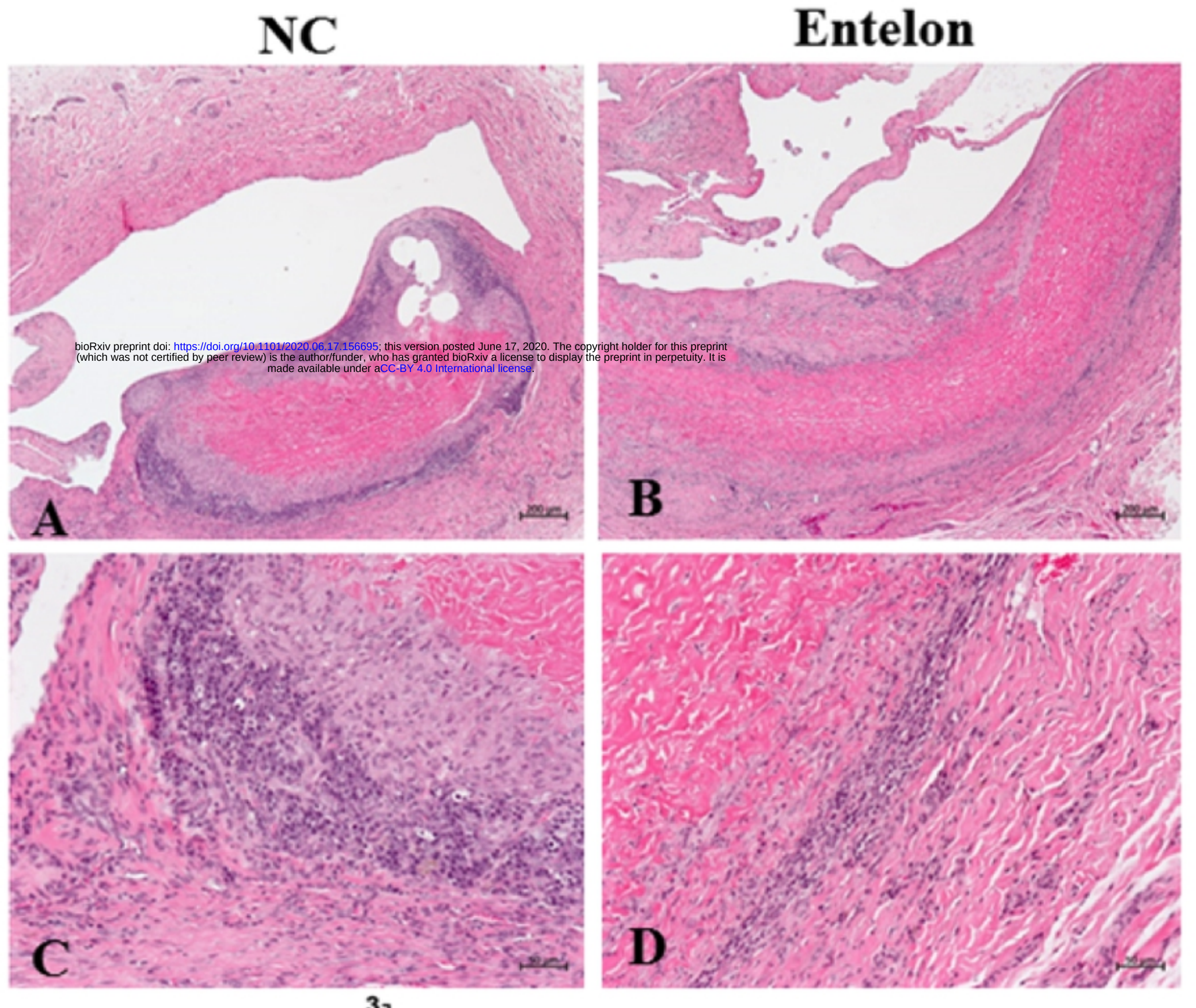

Figure 6

Figure 7